International Journal of Applied Engineering Research ISSN 0973-4562 Volume 13, Number 7 (2018) pp. 4871-4877

Effect of Exfoliated Graphene Defects on Thermal Conductivity of Water Based Graphene Nanofluids

A. Arifutzzaman
PhD candidate, Research Assistant,
Department of Manufacturing and Materials Engineering,
Faculty of Engineering,
International Islamic University Malaysia (IIUM),
P.O. Box 10, 50728 Kuala Lumpur, Malaysia

A. A. Khan
Professor, Department of Manufacturing and Materials Engineering,
Faculty of Engineering,
International Islamic University Malaysia (IIUM),
P.O. Box 10, 50728 Kuala Lumpur, Malaysia

A. F. Ismail
Professor, Department of Mechanical Engineering,
Faculty of Engineering,
International Islamic University Malaysia (IIUM),
P.O. Box 10, 50728 Kuala Lumpur, Malaysia

M. Z. Alam
Professor, Department of Biotechnology Engineering,
Faculty of Engineering,
International Islamic University Malaysia (IIUM),
P.O. Box 10, 50728 Kuala Lumpur, Malaysia

I. I. Yaacob
Professor, Department of Manufacturing and Materials Engineering,
Faculty of Engineering,
International Islamic University Malaysia (IIUM),
P.O. Box 10, 50728 Kuala Lumpur, Malaysia

Abstract

In this work, sonication assisted exfoliated Graphene (Gr) was separated into five different suspensions using a systematic centrifugation scheme (4000-500 rpm) for the two different solvents N-Methyl-2-Pyrrolidone (NMP) and N, N-dimethylformamide (DMF). Gr dispersions in deionized water (DW) were prepared by the re-dispersion process with the aid of vacuum filtration. Systematic thermal conductivity (TC) measurements were conducted separately on the prepared Gr dispersion in DW with rising temperature ranging from 25 to 60 ºC. Defects in exfoliated Gr samples were identified in terms of intensity ratio of D and G band (I_D/I_G) of Raman spectroscopy. For a fixed time of sonication values of I_D/I_G were found considerably higher in higher centrifugation speed (rpm). This phenomenon was perceived for both of the solvents. However, obtained values of I_D/I_G for the exfoliated Gr in NMP (Gr-NMP) were lower than that of Gr exfoliated by DMF (Gr-DMF). Lowest values of I_D/I_G found for 500 rpm, were 0.697 and 0.879 for the Gr-NMP and Gr-DMF respectively. Effect of exfoliated Gr defects were evaluated on the TC of Gr dispersed DW nanofluids. At 60 ℃, TC of Gr-NMP dispersion in DW was obtained 1.146 W/m-K for I_D/I_G of 0.697 (500 rpm) and 0.935 W/m-K for I_D/I_G of 0.916 (4000 rpm). Similarly occurrence was also apparent for the Gr-DMF dispersion in DW.

Keywords: exfoliation, graphene defects, Raman spectroscopy, thermal conductivity, nanofluids and percentage enhancement.

INTRODUCTION

Graphene (Gr) is one or several planar sheets of carbon atoms. It possesses unique physical and chemical properties, extensively high thermo-electrical conductivity as well as enormously large surface area. Presence of edges in Gr nanosheets is the main feature that makes difference from CNTs and other carbon materials [1]. Chemical processing such as liquid-phase exfoliation (LPE) of graphite has shown the most anticipation to produce Gr suspension in organic solvents [2, 3, 4, 5, 6]. Microcrystalline graphite particles can exfoliate into separate Gr flakes in the solvent with the aid of sonication by generating the shear forces and cavitation in solvent [7, 8]. The matching of surface energy of Gr and solvent is one of the most prominent criterions for a successful exfoliation process [5]. Surface energies of solvent NMP or DMF are closely matched with the graphite required for successful exfoliation to Gr sheets [9]. Sedimentation-based separation approach could divide the suspended flakes on the basis of degree of sedimentation due to the effect of centrifugal force on the flakes [10]. Suitable range of centrifugation speeds is identified from 4000rpm to 500rpm for the analysis of sonication assisted exfoliated Gr [11].

Gr nanoribbons are subject to edge disorder due to the high reactivity of the edges. Defects in Gr flakes are categorized as in plane defects or point defects in the basal plane and boundary defects or edge defects. Ruiz, et al., (2011) [12] found that exfoliation creates the boundary defects in the Gr flakes. Lotya, et al., (2009) [4] and Ciesielski and Samorì, (2014) [6] also confirmed that defects in exfoliated Gr flakes are predominantly located at the edges of the Gr flakes and the basal plane of the flakes is relatively defect free. Casiraghi, et al., (2009) [13] and Ferrari, (2007) [14] carried out a detailed

Raman investigation on Gr flakes with well-defined edges oriented at different crystallographic directions. They found that, D peak in the Raman spectrum detects the edge defects in Gr sheets where, intensity of D peak indicates the degree of edge defects in Gr. D to G peak intensity ratio is never null for Gr due to some disorder at the edges [15]. As the geometrical quality of the Gr edges are difficult to control even in the case of the ultra-smooth Gr nanoribbons obtained by the most effective and innovative techniques [16, 17].

Several number of nanostructured materials have been produced with the aid of modern material process and synthesis technologies. A wide variety of thermal properties are obtained from the equivalent bulk materials. Thermal conductivity (TC) is considered to be most important parameter accountable for the enhanced heat transfer [18]. Thermal transport properties are important for understanding the effect of controlled defects on exfoliated Gr. Theoretically, it has been calculated that, TC of Gr sheet intensely depended on the intensity of edge chirality of Gr sheets [19]. Hu, et al., 2009 [17] found considerable decrease in TC using classical molecular dynamics for rough edged Gr nanoribbons compared to the perfect Gr nanoribbons. It is control by the edge phonon scattering mechanism [20]. Numerically analysis illustrated that edge roughness can destroy TC. Ballistic flow of phonons is suppressed considerably in the case of rough edges being replaced by the energy super diffusion [1].

With the comparison of modern nanotechnology and orthodox thermal science, nanofluids are offering significant potential in heat transfer area as enhanced thermal transport media. Yu, et al., (2010) [21] experimentally witnessed the enhanced TC of Gr nanosheets containing nanofluids. As heat transport through the Gr plane is anticipated to be the major influence for the enhancement of TC. Baby and Ramaprabhu, (2011) [22] synthesized thermally exfoliated Gr nanofluid and obtained an enhancement in TC over the base fluid. Gu et al., (2014) [23] have used Gr filler in polymer matrix composite. It was found higher enhancement in TC compare to the orthodox thermal conductive fillers. Therefore, investigations of TC of Gr nanosheets suspended nanofluids provide a significant potential and regarded as an attractive candidate for next-generation materials for in heat transfer application [21, 24].

Although researchers have conducted some theoretical studies on the edge defect engineering in order to explain the transport properties of Gr sheets. Several studies available in literature shown that, the various physical and chemical factors have been proposed to play their respective vital roles on the heat transfer behaviors of nanofluids such as size, shape and the species of the nanoparticles along with the volume fraction and temperature of nanofluids. Till known, there is no work has been conducted regarding the analysis of exfoliated Gr defects effects on the TC of Gr suspended nanofluids. Therefore, the objective of this work is to investigate the effects of defects in exfoliated Gr on TC enhancement of exfoliated Gr suspended DW nanofluids. The influencing factors including, temperature, centrifugation speeds and exfoliation solvents are also analyzed.

METHODS MATERIALS AND METHODS

Production of Gr

200 mg of graphite powder and 200 ml of NMP solvent (Fisher Scientific (M) Sdn. Bhd) was mixed in a beaker and exfoliated by bath sonication (model: 3510E-MTH, 100W, 42kHz) for 3 hours. After exfoliation process first prepared dispersion was centrifuged at 4000 rpm for 45 minutes using eppendorf Centrifuge 5804. Larger flakes were tending to sediment at the bottom of the centrifuge tube. Supernatant of Gr in NMP was decanted from the sediment by take away of top ~ 80% of the dispersion by pipette without disturbing the sedimentation. Separated supernatant dispersion was then preserved into the other tube for characterization. Then 16 ml of NMP was added into the sedimentation and re-dispersed by a mild sonication of 15 minutes and centrifuged with 3000rpm for 45 minutes. Supernatant of Gr in NMP was decanted again from sediment by take away of top ~ 80% of the dispersion. This procedure was further repeated for three times, centrifuging the re-dispersed sediment at 2000, 1000 and 500 rpm, after every time separating the supernatant. After 500 rpm centrifugation, the procedure was stopped as 500 rpm is the minimum required to remove un-exfoliated graphitic crystal [6, 10, 11]. Each of the supernatant suspensions was the product. Same procedure was repeated for the solvent DMF with maintaining all the parameters and conditions same. During the experiment water level was maintained carefully at the exact position in the water bath sonicator. Dispersion concentration of the suspension was estimated by UV-vis (Thermo Scientific, Multiskan GO) absorbance spectroscopy analysis. Field Emission Scanning Electron Microscopy, FESEM (Model JEOL JSM-6700F) was used to examine the morphology of the as prepared exfoliated Gr sheets. Raman spectroscopy (InVia Reflex, Renishaw, UK) of exfoliated Gr was performed on the prepared films on silicon wafer. Spectra were recorded with 514 nm excitation, within the Raman shift from 1000 to 3200 cm^{-1} incorporating with the WiRE 4 software.

Preparation of Gr dispersed DW nanofluids

The organic solvent was removed from Gr nanosheets using vacuum filtration. Then it was re-dispersed into DW. Gr suspensions in DW were bath sonicated for 15 min and then stirred about 1hr using magnetic stirrer. Exfoliated Gr in respective organic solvents is denoted as Gr-'solvent'. It means, Gr exfoliated in solvent NMP and DMF are expressed as Gr-NMP and Gr-DMF respectively.

Thermal conductivity measurements

Thermal conductivity (TC) of the nanofluids were measured using a KD2 Pro thermal properties analyser (Decagon, USA, version 5), built on the principle of transient hot-wire technique. The KS-1 single-probe sensor was used for these measurements. The accuracy of the instrument is specified by the manufacturer to be within ±5%. A modern programmable refrigerated water bath of Model AD07R-40-12E, Polyscience, USA, was used for controlling the temperature. It

is able to maintain temperature uniformity within ±0.01 ºC. Instead of monitoring the temperature of the bath, a thermocouple was positioned inside the sample to monitor the sample temperature [25]. Sensor performance was measured with fluid glycerol (recommended and supplied by manufacturer). About 45 ml of sample was taken into a close vial. Sensor probe was completely plunged vertically into the sample. The schematic explanation of TC arrangement is presented in Figure 1. The deviation of the measured temperature was considered around ± 0.5 ºC. All measurement was conducted within the same range of temperature 25 to 60 ºC. Data was taken for every temperature after getting complete equilibrium state. Each data was repeated minimum 10 times (up to 25 times) for the precision purpose. Absolute errors of all measurements were found ±0.001. Almost 20% of data were ignored considering them as outliers. Average values were taken for the analysis. After the above-mentioned careful check on the measurement condition and procedure, it gains strong confidence on the experimental results.

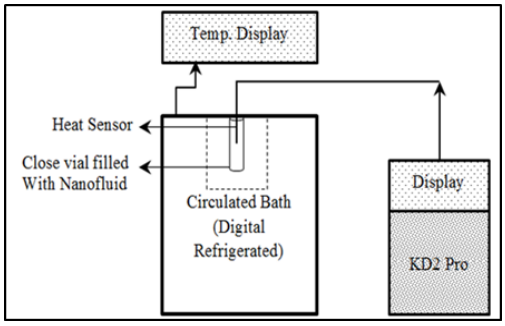

Figure 1: Schematic illustration of TC measurement instrument.

RESULTS AND DISCUSSIONS

Characterization of exfoliated Gr

Gr dispersions in DW

After production of Gr using sonication assisted exfoliation, suspension's concentration for varying centrifugation rates (rpm) were estimated from the absorbance analysis of prepared standard graphs with the identified absorption coefficients. Concentration was obtained lower for lower rpm samples. As, sedimentation-based separation approach using controlled centrifugation divides the suspended Gr flakes on the basis of degree of accumulation due to the effect of centrifugal force on the Gr flakes [10]. To investigate effect of defects on exfoliated Gr five different samples of Gr-NMP dispersion in DW were prepared with centrifuge speed of 4000, 3000, 2000, 1000 and 500 rpm. Every sample was maintained in same concentration (0.095 mg/ml). To see the effect of solvent on the TC of Gr suspension in DW, five different samples of Gr-DMF/DW were also prepared for the centrifuge speed of 4000, 3000, 2000, 1000 and 500 rpm. For the compression purpose same concentration (0.095 mg/ml) was maintained in all samples. Figure 2 shows the physical appearance of the Gr suspensions in DW. Digital photographs in Figure 2a and 2b show the representative of Gr suspension in DW samples of 500 rpm after preparation of 30 days for the Gr exfoliated by the solvent NMP and DMF respectively. A homogeneous and uniform dispersion is acquired. It was apparent that there was no sedimentation in the solutions.

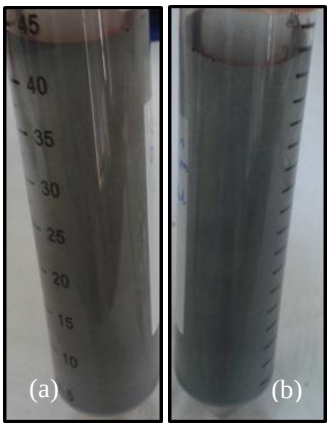

Figure 2: Physical appearance of the dispersion of exfoliated Gr in DW for the representative sample of 500 rpm centrifugation produced in: (a) NMP and (b) DMF.

Electron microscopy

Figure 3 shows the representative FESEM images of as produced exfoliated Gr sheets of the samples separated by centrifugation speed 500 rpm. Images show that the few layers of Gr flakes. Figure 3a and 3b mentioning the samples of Gr-NMP and Gr-DMF respectively. It is speculated that the flake size is approximately similar for both of the exfoliated Gr in NMP and DMF solvents for the same exfoliation condition with the same precursor graphite powder. FESEM analyses of the exfoliated samples revealed the presence of number of flakes stacking. It can be seen that most of the exfoliated flakes are very thin and Gr layers are stacked one over another in an ordered manner [8].

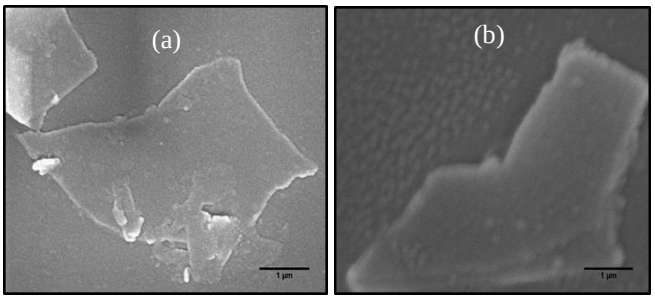

Figure 3: FESEM images of Gr flakes (a) Gr-NMP and (b) Gr-DMF. Representative of exfoliated Gr samples for 500 rpm.

Raman spectroscopy

Representatives of Raman spectrum measured on the precursor graphite powder and samples of exfoliated Gr in DMF and NMP solvents for final centrifuge speed 500 rpm are shown in Figure 4. The spectrum for the starting precursor powder is presented for the comparison purpose. Three characteristic peaks in the Raman spectra of carbon materials

are appeared. In the measured Raman spectrum on precursor Graphite powder (PGP) G-band has been found at ~ 1578.73 cm^{-1}, 2D-band at ~ 2648.96 cm^{-1} and D-band at ~1311 cm^{-1}. G band position for exfoliated Gr samples by NMP and DMF (supernatant of 500 rpm centrifugation) have been shifted to ~ 1583.64cm^{-1} and ~1582.59 cm^{-1} respectively. It reveals the transformation of Gr form the graphite flakes by LPE. Increases in Raman shift (cm^{-1}) of G-band form the precursor graphite is the indication of conversion of graphite to Gr sheets [26]. The sharp G-band is appearing around 1583 cm^{-1} in the spectrum of Gr, for the in-plane vibrational of sp2 hybridized carbon atoms that comprise the Gr sheet [26, 27, 28].

2D-band of these Gr samples has been found at ~ 2646.47 cm^{-1} and 2636.79 cm^{-1} respectively. Although the shapes are similar for the 2D-bands, however there are some obvious differences in the FWHM which could estimate the number of Gr layers [29]. FWHM of 2D-band peak for both of the NMP and DMF exfoliated samples is detected about 66 cm^{-1} which recommends the presence of about five-layer Gr in the representative analyzed samples [29].

It is noted that the starting Graphite powder displays a smaller defect. Defect level can be quantifying by the relative intensity of D and G band intensity, i,e by ratio I_D/I_G [4]. As shown in Figure 4, I_D/I_G for the precursor graphite powder is obtained 0.599. Values of I_D/I_G are found 0.879 and 0.697 for the exfoliated Gr by solvent DMF and NMP respectively for the representative 500 rpm centrifuge samples. This larger D band intensity of exfoliated Gr than the starting graphite powder indicating that processing induces edge defects [4]. It also reveals the formation of Gr from the graphite by exfoliation [10].

The D-band intensity provides the evidence of presence of edge defects in Gr sheets [30, 31]. Ring breathing mode from sp2 carbon rings represents the D band, the disorder or the defect band. The ring must be near a Gr edge or a defect to be active. It could be attributed to the inelastic scattering originated from the disordered Gr edges [13]. This band is generally weaker in graphite then its transformed Gr [26]. For exfoliated Gr, a large intensity of the disorder-induced peak is evident. Due to the short time sonication and the non-oxidative nature of the solvent mixture, the formation of basal defects can be excluded [32]. Moreover, sonication of graphite is considered as a nondestructive process [4]; therefore defects are predominantly located at the edges of the Gr flakes and the basal plane of the flakes is relatively defect free [4, 6].

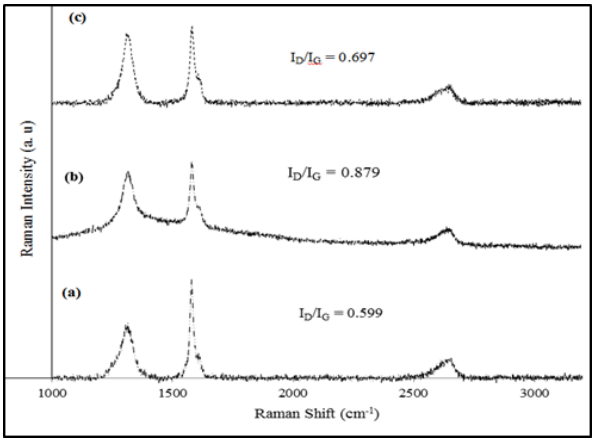

Figure 4: Raman spectra of (a) graphite powder (LPE precursor), exfoliated Gr samples of 500 rpm centrifuge: (b) G-DMF and (c) Gr-NMP.

Defect content in exfoliated Gr

It must consider the defect content of the exfoliated Gr. Ratio of D and G band intensity, I (I_D/I_G) is plotted as a function of centrifugation rate (rpm) in Figure 5. Y-axis error bars come from the standard deviation of average values of measurements at different points on the prepared films on Si wafer. For exfoliation using NMP solvent presents in left y-axis in Figure 5. Ratio of I_D and I_G is found 0.916 for 4000 rpm centrifugation. Reduced values of I_D/I_G are found with decreasing centrifuge rate. Values of I_D/I_G are 0.832, 0.798, 0.761 and 0.697 for 3000, 2000, 1000 and 500 rpm respectively.

Evolution of D-peak in Raman spectrum is due to the defects associated in the edges of Gr flakes [4, 10, 11, 33, 34]. Defects being formed are associated with new edges [4, 33]. It means that the total edge length is increased for smaller Gr flakes [10]. Moreover, edge defects are incorporated during the processing as sonication cuts the initially large crystallites up into smaller flakes. These smaller flakes have more edges per unit mass resulting in an increase in edge defect population [4]. Small flakes have been separated by the higher centrifuge rate [11]. For this reason, for a fixed time of sonication I_D/I_G increases considerably with centrifugation speed, demonstrating that the flakes retained at higher rotation rates have more defects [10, 11].

Same graphite powder has been exfoliation by maintaining the same parameters for the different solvent environment using DMF. In this case it is also found the increase in I_D/I_G with increasing rpm presented in right y-axis Figure 5. These ratios are obtained 1.340, 1.143, 1.022, 0.944 and 0.879 for the centrifugation rate 4000, 3000, 2000, 1000 and 500 rpm respectively. Notably it needs to be mentioned that the obtained values of I_D/I_G for the exfoliated Gr from NMP solvent is lower than that of Gr exfoliated by DMF solvent. Formation of defects in Gr sheets vary for the solvents used in exfoliation [34]. D peak in Raman spectra is not governed by the sonication induced damage of Gr flakes. However,

covalent attachment of solvent molecules to Gr edges is responsible for evolution and increase of D peak. These covalent bonds are excessive in high dielectric constant (k) solvent exfoliated Gr flakes compared to the low k solvents exfoliated Gr [34].

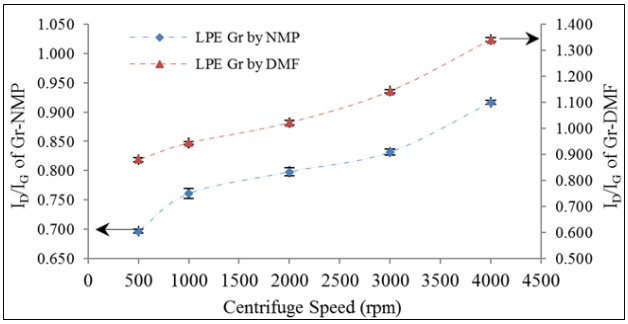

Figure 5: Ratio of Raman D and G band intensity of exfoliated Gr as a function of final centrifugation speed (rpm) for: Gr-NMP in left Y-axis and Gr-DMF in right Y-axis.

Thermal conductivity of Gr dispersed DW nanofluids

The heat in Gr mostly carried by acoustic (A) phonons rather than by electrons, while optical (O) phonon [28] modes are not active for the conduction of heat in Gr [35]. On the other hand, D band in Raman spectrum on Gr comes from broken or incomplete hexagonal rings at the edges for the optical phonons [14]. For this reason, it leads to speculate that increase of D band intensity due to the increase optical (O) phonons scatter is the reason for limiting the TC of Gr. Figure 6 illustrates the effect of D peak intensity on the TC of Gr suspensions in DW. Figure 6a and 6b describe the TC, K_{nf} of Gr-NMP and Gr-DMF suspension in DW (Gr-NMP/DW and Gr-DMF/DW) as a function of intensity ratio of D and G band (I_D/I_G) of Raman spectrum for the samples of corresponding increasing centrifuge speed (rpm). Four graphs are shown for the measured K_{nf} at four different temperatures of 25, 40, 50 and 60 ℃. Y-axis error bars are the errors with the K_{nf} measurements of both Gr-NMP/DW and Gr-DMF/DW samples.

It shows that in both graph that, in all the temperature K_{nf} is higher in lower I_D/I_G. At 25 ℃ thermal conductivities are obtained 0.748, 0.695, 0.684, 0.671 and 0.662 W/m-K for the Gr-NMP/DW samples with the I_D/I_G of 0.697, 0.761, 0.798, 0.832 and 0.916 respectively (Corresponding centrifugation speed 500, 1000, 2000, 3000 and 4000 rpm respectively) (Figure 6a). While, thermal conductivities at 25 ℃ for Gr-DMF/DW are obtained 7.092, 0.671, 0.618, 0.642 and 0.626 W/m-K, for I_D/I_G of 0.879, 0.944, 1.022, 1.143 and 1340 respectively (Figure 6b). At 40 ℃ temperature K_{nf} of Gr-NMP/DW is also reduced from 0.858w/m-K (I_D/I_G: 0.679) to 0.693 W/m-K with the I_D/I_G of 0.916 for the 4000 rpm sample. Similar trends of K_{nf} reduction are also shown for higher temperature 50 and 60 ℃ for both of the samples Gr-NMP/DW and Gr-DMF/DW. At 60 ℃ temperature, K_{nf} of Gr-NMP/DW is perceived 1.146 W/m-K with I_D/I_G of 0.697 (500 rpm) and 0.935 W/m-K for I_D/I_G of 0.916 (4000 rpm). Whereas, at 60 ℃, K_{nf} of Gr-DMF/DW sample is reduced to 0.832 from 1.081 W/m-K for I_D/I_G reduced to 0.879 (for 500 rpm) to 1340 (for 4000 rpm).

Edge roughness in the Gr nanosheets suppresses the TC, K_{nf} [1, 17]. This effect is associated by two orders of magnitude one is the edge-induced energy localization and another one is the suppression of the phonon transport [1]. Moreover, ballistic flow of phonons is suppressed considerably in the case of defective edged Gr nanosheets which being replaced by the energy super-diffusion [36]. Ring breathing mode from sp2 carbon rings represents the D band in Raman spectrum, the disorder or the defect band. The ring must be near a Gr edge or a defect to be active. It could be attributed to the inelastic scattering originated from the disordered Gr edges [13, 34]. In LPE technique higher centrifuge speeds (rpm) provide higher edge defects [10]. It is also found experimentally as shown in Figure 5. Moreover, inelastic phonon-phonon scattering, which is responsible for the thermal resistance and two unique features that contribute to the enormously large TC of suspended Gr. Thermal transport properties of Gr has limited by intrinsic properties of the Gr lattice, which is crystal anharmonicity [37]. On the other hand, extrinsic effects such as phonon-boundary or defect scattering have prominent effects on limiting the thermal transport properties of Gr [38].

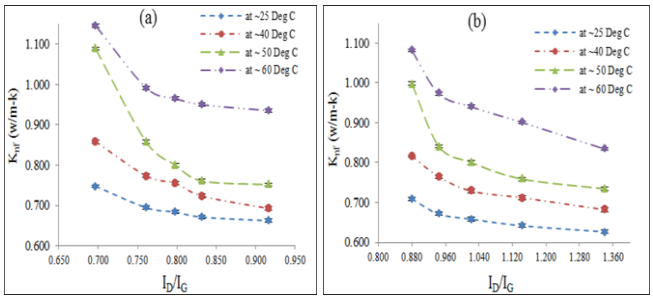

Figure 6: Thermal conductivity verses intensity ratio of D and G band (I_D/I_G) for four different temperatures at 25, 40, 50 and 60 ℃: (a) Gr-NMP/DW and (b) Gr-DMF/DW.

Figure 7a and 7b illustrate the percentage thermal conductivity enhancements (PTCE) of Gr-NMP/DW and Gr-DMF/DW samples respectively with the varying temperature. Five plots are presented for the samples of 4000, 3000, 2000, 1000 and 500 rpm respectively (with representing the I_D/I_G). In graphs, I_D/I_G is presented as short form D/G with the corresponding centrifuge speeds. PTCE is calculated using the relation, $\eta = [(K_{nf}-K_{bf})/K_{bf}) \times 100\ \%]$ where, K_{nf} and K_{bf} are the TC of Gr suspensions in DW and base fluid DW respectively.

For the 4000 rpm Gr-DMF/DW sample (Figure 7b) PTCE's are obtained about 4.5, 9, 15 and 30 % at 25, 40, 50 and 60 ℃ temperature respectively, while these percentages are found about 9, 9.5, 18 and 44 % for 4000 rpm Gr-NMP/DW sample at the same temperatures respectively (Figure 7b). Nearly similar trends have been perceived for the samples of 3000,

2000 and 1000 rpm. However, PTCE of 500 rpm sample is found higher than that of the other samples with successfully higher rpm samples. This phenomenon is occurred for both of the Gr-NMP and Gr-DMF (Figure 7a and 7b). At room temperature PTCE is attained about 17 and 24 % for the 500 rpm samples of Gr-DMF/DW and Gr-NMP/DW respectively. These percentages are increased to be 67 and 77 % at 60 ºC for the Gr-DMF/DW and Gr-NMP/DW respectively.

Above explanation reveals few specific points. First, TC of Gr suspension in base fluid has the dependency on temperature which is evidenced in all samples for both of Gr-DMF/DW and Gr-NMP/DW. Temperature dependent TC is individual which is apart from the effect of edge defects of the Gr. Secondly, in these samples; it is perceived that the PTCE's are higher for the Gr-NMP/DW than that of the Gr-DMF/DW samples. This phenomenon is apparent in all the measured temperature. It is assumed that these variations of TC enhancements are occurred due to the difference of degree of edge defects in the Gr samples. Exfoliated Gr-NMP of all centrifugation speeds exhibit lower degree of defects (I_D/I_G) than Gr-DMF. Experiments are conducted via same protocol with same parameters of the exfoliation from the same precursor graphite only changing the solvent. Thirdly, TC enhancement of 500 rpm samples is found comparatively higher among the all analyzed samples of successive higher rpm. This phenomenon is occurred for both of the Gr-NMP and Gr-DMF.

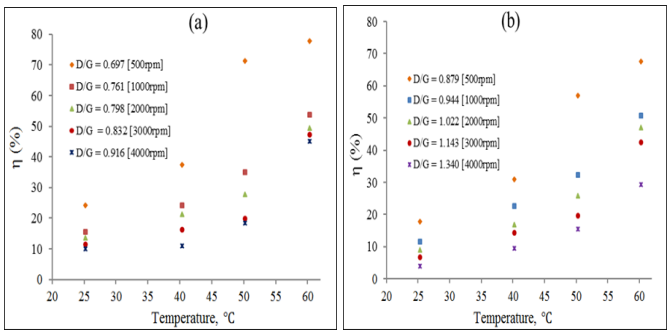

Figure 7: Percentage thermal conductivity enhancements (PTCE) as a function of temperature for the samples of 4000, 3000, 2000, 1000 and 500 rpm respectively (with representing the I_D/I_G): (a) Gr-NMP/DW and (b) Gr-DMF/DW.

CONCLUSIONS

The study shows that, few layers of Gr flakes were effectively fabricated using sonication assisted LPE separately in two different solvent NMP and DMF. Analysis of Raman spectroscopy reveals that the values of I_D/I_G for a fixed time sonication (for both solvents) were perceived significantly higher in higher rpm, demonstrating that the flakes retained at higher rotation rates have more defects. Due to the effect of Gr edge defects, TC of 500 rpm samples exhibited the maximum TC compared with the successively higher centrifuge speeds. It is perceived in all measured temperature varying for both of Gr-NMP/DW and Gr-DMF/DW nanofluid samples. It is also concluded that, Gr-NMP/DW showed higher PTCE over the base fluid (at 60 ℃ ~77.5% for 500rpm) than that (at 60 ℃ ~67.5% for 500rpm) of Gr-DMF/DW.

ACKNOWLEDGEMENTS

Authors are grateful to the Research Management Centre (RMC), International Islamic University Malaysia (IIUM) for all kinds of support to accomplish this research work. Authors also courteously acknowledge the financial support provided by the Ministry of Higher Education (MOHE) under research grant ERGS 12-020-0020.

REFERENCES

[1] A. V. Savin, Y. S. Kivshar and B. Hu. "Suppression of thermal conductivity in graphene nanoribbons with rough edges", *Physical Review B*, vol. 82(19), pp. 195422, 2010.

[2] J. I. Paredes, S. Villar-Rodil, P. Solís-Fernández, M. J. Fernández-Merino, L. Guardia, A. Martínez-Alonso and J. M. D. Tascón. "Preparation, characterization and fundamental studies on graphenes by liquid-phase processing of graphite", *Journal of Alloys and Compounds*, vol. 536, pp. S450-S455. 2012.

[3] J. N. Coleman. "Liquid exfoliation of defect-free graphene", *Accounts of chemical research*, vol. 46(1), pp. 14-22, 2012.

[4] M. Lotya, Y. Hernandez, P.J. King, R. J. Smith, V. Nicolosi, L. S. Karlsson and G. S. Duesberg. "Liquid phase production of graphene by exfoliation of graphite in surfactant/water solutions", *Journal of the American Chemical Society*, vol. 131(10), pp. 3611-3620, 2009.

[5] Y. Hernandez, V. Nicolosi, M. Lotya, F. M. Blighe, Z. Sun, S. De, S. Krishnamurthy, R. Goodhue, J. Hutchison, V. Scardaci, A. C. Ferrari and J. N. Coleman. "High-yield production of graphene by liquid-phase exfoliation of graphite", *Nature Nanotechnology*, vol. 3(9), pp. 563-568, 2008.

[6] A. Ciesielski and P. Samorì. "Graphene via sonication assisted liquid-phase exfoliation", *Chemical Society Reviews*, vol. 43(1), pp. 381-398, 2014.

[7] Y. Arao, Y. Mizuno, K. Araki and M. Kubouchi. "Mass production of high-aspect-ratio few-layer-graphene by high-speed laminar flow", *Carbon*, vol. 102, pp. 330-338, 2016.

[8] S. Vadukumpully, J. Paul and S. Valiyaveettil. "Cationic surfactant mediated exfoliation of graphite into graphene flakes", *Carbon*, vol., 47(14), pp. 3288-3294, 2009.

[9] O. C. Compton and S. T. Nguyen. "Graphene Oxide, Highly Reduced Graphene Oxide, and Graphene: Versatile Building Blocks for Carbon-Based Materials", *Small*. Vol. 6(6), pp. 711-723, 2010.

[10] U. Khan, A. O'Neill, H. Porwal, P. May, K. Nawaz and J. N. Coleman. "Size selection of dispersed, exfoliated

graphene flakes by controlled centrifugation", *Carbon*, vol. 50(2), pp. 470-475, 2012.

[11] U. Khan, A. O'Neill, M. Lotya, S. De and J. N. Coleman. "High-Concentration Solvent Exfoliation of Graphene", *Small*, vol. 6(7), pp. 864-871, 2010.

[12] C. S. Ruiz-Vargas, H. L. Zhuang, P. Y. Huang, A. M. van der Zande, S. Garg, P. L. McEuen and ...J. Park. "Softened elastic response and unzipping in chemical vapor deposition graphene membranes", *Nano letters*, vol. 11(6), pp. 2259-2263, 2011.

[13] C. Casiraghi, A. Hartschuh, H. Qian, S. Piscanec, C. Georgi, A. Fasoli, ... and A. C. Ferrari. 2009. "Raman spectroscopy of graphene edges", *Nano letters*, vol. 9(4), pp. 1433-1441, 2009.

[14] A. C. Ferrari. "Raman spectroscopy of graphene and graphite: disorder, electron-phonon coupling, doping and nonadiabatic effects", *Solid state communications*, vol. 143(1), pp. 47-57, 2007.

[15] L. M. Malard, M. A. Pimenta, G. Dresselhaus and M. S. Dresselhaus. "Raman spectroscopy in graphene", *Physics Reports*, vol. 473(5), pp. 51-87, 2009.

[16] X. Li, G. Zhang, X. Bai, X. Sun, X. Wang, E. Wang and H. Dai. "Highly conducting graphene sheets and Langmuir–Blodgett films", *Nature nanotechnology*, vol. 3(9), pp. 538-542, 2008.

[17] J. Hu, X. Ruan and Y. P. Chen. "Thermal conductivity and thermal rectification in graphene nanoribbons: a molecular dynamics study", *Nano letters*, vol. 9(7), pp. 2730-2735, 2009.

[18] P. Mukesh Kumar, J. Kumar, R. Tamilarasan, S. Sendhilnathan and S. Suresh. "Review on nanofluids theoretical thermal conductivity models", *Engineering Journal*, vol. 19(1), pp. 67-83, 2015.

[19] D. L. Nika, E. P. Pokatilov, A. S. Askerov and A. A. Balandin. "Phonon thermal conduction in graphene: Role of Umklapp and edge roughness scattering", *Physical Review B*, vol. 79(15), pp. 155413, 2009.

[20] W. J. Evans, L. Hu and P. Keblinski. "Thermal conductivity of graphene ribbons from equilibrium molecular dynamics: Effect of ribbon width, edge roughness, and hydrogen termination", *Applied Physics Letters*, vol. 96(20), pp. 203112, 2010.

[21] W. Yu, H. Xie and W. Chen. "Experimental investigation on thermal conductivity of nanofluids containing graphene oxide nanosheets", *Journal of Applied Physics*, vol. 107(9), pp. 094317, 2010.

[22] T. T. Baby and S. Ramaprabhu. "Synthesis and nanofluid application of silver nanoparticles decorated graphene", *Journal of Materials Chemistry*, vol. 21(26), pp. 9702-9709, 2011.

[23] J. Gu, C. Xie, H. Li, J. Dang, W. Geng and Zhang. "Thermal percolation behavior of graphene nanoplatelets/polyphenylene sulfide thermal conductivity composites", *Polymer Composites*, vol., 35(6), pp. 1087-1092, 2014.

[24] T. T. Baby and S. Ramaprabhu. "Investigation of thermal and electrical conductivity of graphene based nanofluids", *Journal of Applied Physics*, vol. 108 (12), pp. 124308, 2010.

[25] D. Decagon. "KD2 Pro Theory", KD2 Pro User Manual, 2006.

[26] J. Hodkiewicz. "Characterizing graphene with Raman spectroscopy", *Thermo Scientific application note*, pp. 51946, 2010.

[27] M. Wojtoniszak, X. Chen, R. J. Kalenczuk, A. Wajda, J. Lapczuk, M. Kurzewski and ... E. Borowiak-Palen. "Synthesis, dispersion, and cytocompatibility of graphene oxide and reduced graphene oxide", *Colloids and Surfaces B*, Biointerfaces, vol. 89, pp. 79-85, 2012.

[28] A. C. Ferrari and D. M. Basko. "Raman spectroscopy as a versatile tool for studying the properties of graphene", *Nature nanotechnology*, vol. 8(4), pp. 235-246, 2013.

[29] Y. Hao, Y. Wang, L. Wang, Z. Ni, Z. Wang, R. Wang and ... J. T. Thong. "Probing Layer Number and Stacking Order of Few-Layer Graphene by Raman Spectroscopy", *Small*, vol. 6(2), pp. 195-200, 2010.

[30] X. Jia, J. Campos-Delgado, M. Terrones, V. Meunier and M. S. Dresselhaus. "Graphene edges: a review of their fabrication and characterization", *Nanoscale*, vol. 3(1), pp. 86-95, 2011.

[31] H. S. Wahab, S. H. Ali and A. M. A. Hussein. "Synthesis and Characterization of Graphene by Raman Spectroscopy", *Journal of Materials Sciences and Applications*, vol. 1(3), pp. 130-135, 2015.

[32] D. Tasis, K. Papagelis, P. Spiliopoulos and C. Galiotis. "Efficient exfoliation of graphene sheets in binary solvents", *Materials Letters*, vol. 94, pp. 47-50, 2013.

[33] A. O'Neill, U. Khan, P. N. Nirmalraj, J. Boland and J. N. Coleman. "Graphene dispersion and exfoliation in low boiling point solvents", *The Journal of Physical Chemistry C*, vol. 115(13), pp. 5422-5428, 2011.

[34] P. K. Srivastava and Ghosh. "Defect engineering as a versatile route to estimate various scattering mechanisms in monolayer graphene on solid substrates", *Nanoscale*, vol. 7(38), pp. 16079-16086, 2015.

[35] E. Munoz, J. Lu and B. I. Yakobson. "Ballistic thermal conductance of graphene ribbons", *Nano letters*, vol., 10(5), pp. 1652-1656, 2010.

[36] J. A. Sánchez-Gil, V. Freilikher, I. Yurkevich and A. A. Maradudin. "Coexistence of ballistic transport, diffusion, and localization in surface disordered waveguides", *Physical review letters*, vol. 80(5), p. 948, 1998.

[37] L. Lindsay, D. A. Broido and N. Mingo. "Flexural phonons and thermal transport in graphene, *Physical Review B*, vol., 82(11), PP. 115427, 2010.

[38] A. A. Balandin. "Thermal properties of graphene and nanostructured carbon materials", *Nature materials*, 10(8), pp. 569-581, 2011.